Chapter 3

TEG Hot Side Performance Enhancement using Vortex Generators

Overview: This chapter experimentally investigates advanced hot-side heat transfer enhancement for thermoelectric generators (TEGs). The heat exchanger's rectangular section is divided into computational domains analyzed with a 1-D thermal resistance model. After achieving stable conditions, energy conservation calculations are derived for each domain. The study analyzes how vortex generator geometry, distance-to-height ratio, and inclination angle affect thermohydraulic performance, including the heat transfer coefficient, pressure drop, and thermal enhancement factor. Using hot air, a comparative analysis identifies the optimal vortex generator configuration to maximize thermal efficiency and TEG power output.

3.1 Setup description

The configuration illustrated in Fig. 3.1 encompasses fundamental elements, such as a heat exchanger, a blower, a heater, and a data acquisition system for temperature measurement. The air is blown using a Cheston 500W blower and the HX receives hot air after being heated with a 2kW heater. The flow and air temperature are regulated to mimic the flow of an exhaust gas. Temperature measurements are conducted using a PT100 thermocouple. Fig. 3.2(a) illustrates placements of thermocouples (for internal and surface temperature measurements), tapping for pressure difference measurement, along with the HX inlet and outlet. Fig. 3.2(b) shows the computational model and elucidates the determination of the local heat transfer coefficient. In the thesis, the term control volume refers to the discrete computational domains used in the numerical model to discretize the rectangular flow channel along the direction of the hot air flow (the x-axis).

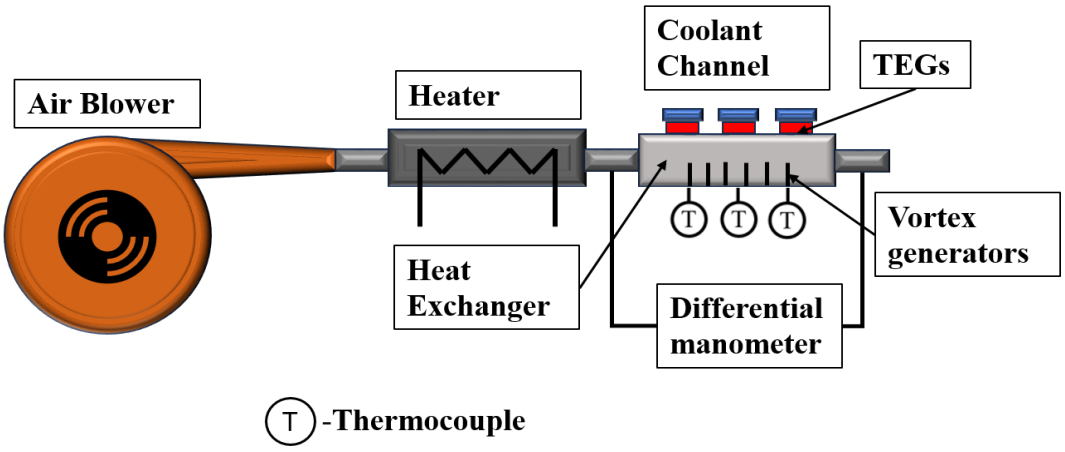

Fig. 3.1 Schematic diagram of the experimental setup

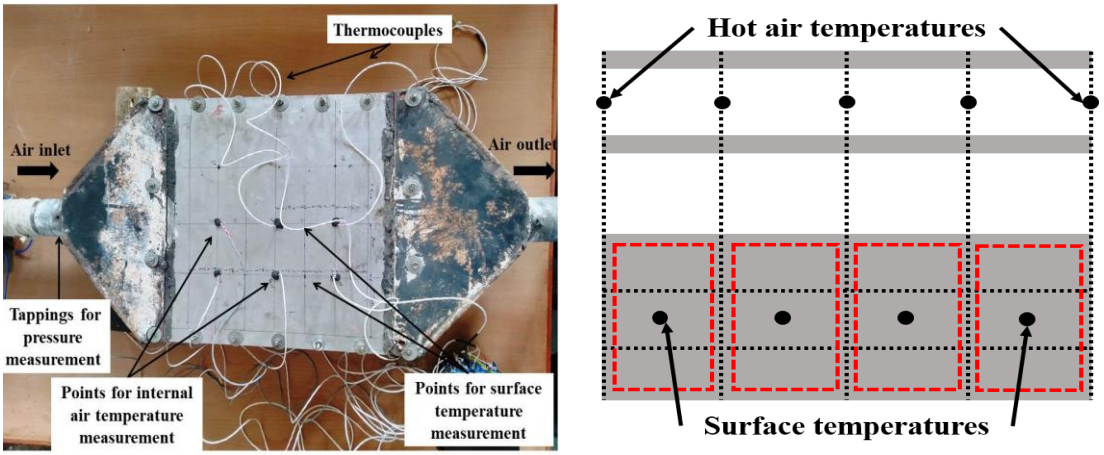

(a) **(b)**

Fig. 3.2 (a) Heat exchanger and placement of thermocouple (b) Division of the heat exchanger into Computational domains

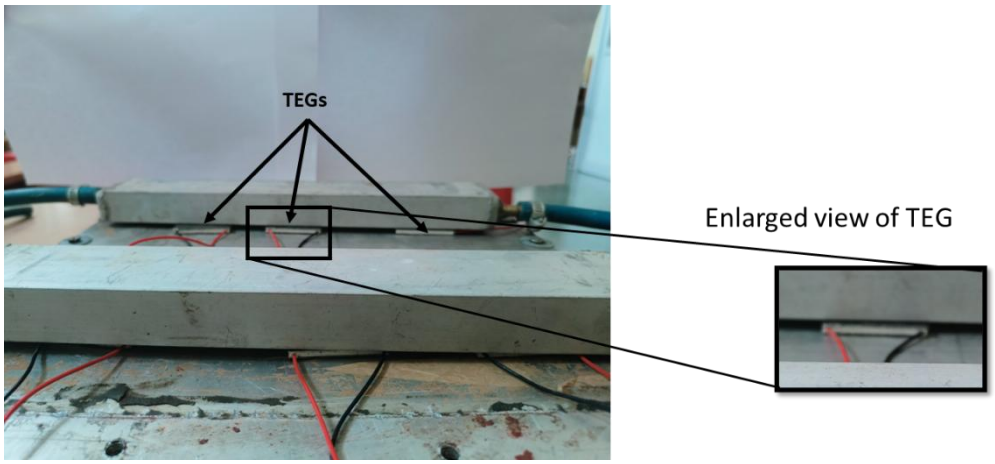

Fig. 3.2 (c) Thermoelectric Generator placement over the heat exchanger

These domains are dimensionless, discrete segments used for numerical analysis and are not thermodynamic control volumes in the classical sense. Additionally, Fig. 3.2(c). depicts TEG configuration.

The heat exchanger consists of three main sections: a diverging section, a rectangular channel, and a converging section. The rectangular section is of particular interest as it serves as the mounting surface for the thermoelectric generators, enabling power generation. The size of the heat exchanger plays a crucial role in waste heat recovery, as an excessively short length would limit the power output of the thermoelectric generators, whereas an overly long heat exchanger would lead to a significant increase in exhaust pumping power. The present uses hot air as the source of waste heat. The hot air properties resemble closely exhaust from an automobile. In the present study, the dimensions of the rectangular section are determined based on the recommendations provided by He et al. (2015), ensuring an optimal balance between power generation and system efficiency. The dimensions of the rectangular part of HX are 25mm (inclusive of plate thickness) in height and 290mm in width. To mitigate pressure-drop effects, the HX's length was constrained to a maximum of 300mm, given its direct correlation to pressure drop. After establishing the proportions of the HX, the selection of construction material became imperative. Aluminum was preferred for its commendable attributes of high thermal conductivity and corrosion resistance as the heat exchanger material. In this study, a modest thermoelectric generator design was employed. The TEG has a dimension of 40mm x 40mm x 3.6mm, it weighed 30gm. The operating temperature of the TEG is from 0°C to 120°C. the open circuit voltage rated by the manufacturer was 4.8V. The experimental setup emulates air as the heated gas enters the heat exchanger, engaging in heat exchange with the thermoelectric generators. The TEG consists of hot and cold sides; the former captivates thermal energy from the outer

face of the HX and transfers it to the thermoelectric generator, which generates electricity. The power generated is directly influenced by the thermal characteristics of HX. Thus, the HX is characterized by a diverging sector, a crucial rectangular canal that accommodates the thermoelectric generators for electricity generation, and a converging sector. The heat dissipated by the heated gas undergoes an equal transfer to both the top and bottom walls of the HX. It is corroborated by the closely matching temperatures (within ±0.2°C) observed on both the lower and upper surfaces of the HX.

3.1.1 Arrangement of VGs

The experimental investigation involves the utilization of three distinct types of vortex generators, namely the envelope (M), delta (D), and fishtail (F), as illustrated in Figs. 3.3(a-c). In the context of the experiment, the HX incorporates an array-style arrangement of vortex generators on its bottom surface, featuring 5 arrays, as depicted in Figs. 3.4(a) and (b). The quantification of VGs in each post is facilitated by the distance-to-height ratio, specified as the separation between consecutive vortex generators within the same column.

The VGs are examined for distance-to-height ratios: 2, 3, and 4. Four angles of inclination, namely 30°, 45°, 60°, and 90°, measured horizontally, are systematically investigated for each specified distance-to-height ratio, as delineated in Fig. 3.5, along with the display of the angle of inclination definition. The envelope and fishtail designs were chosen due to their potential to generate strong and organized vortices,. The delta shape, commonly used in aerospace and heat exchanger applications, was chosen due to its ability to generate longitudinal vortices that enhance thermal performance. In the pursuit of identifying optimal configurations and vortex generator settings, a comprehensive analysis comprising 37 distinct experiments was conducted.

- 1 for heat exchanger without VGs
- 3 for shapes (delta, envelope, and fishtail)
- 3 for D/H ratios (2, 3, and 4)
- 4 of inclination angles (30°, 45°, 60°, and 90°)

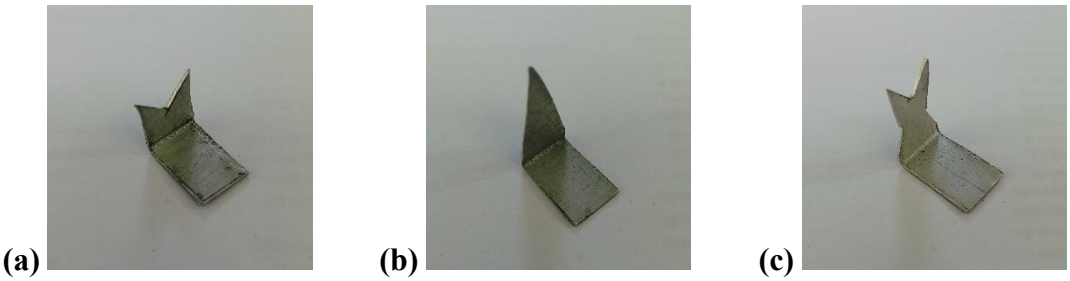

Fig. 3.3 (a) Envelope, (b) Delta, and (c) Fishtail vortex generators

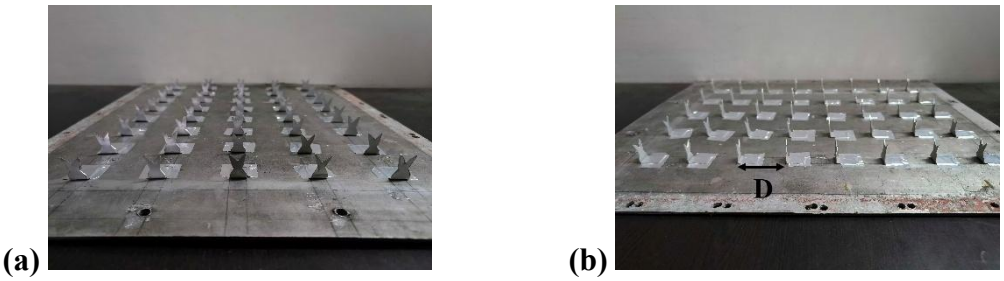

Fig. 3.4 (a) Front view and (b) Side view of VGs arrangement

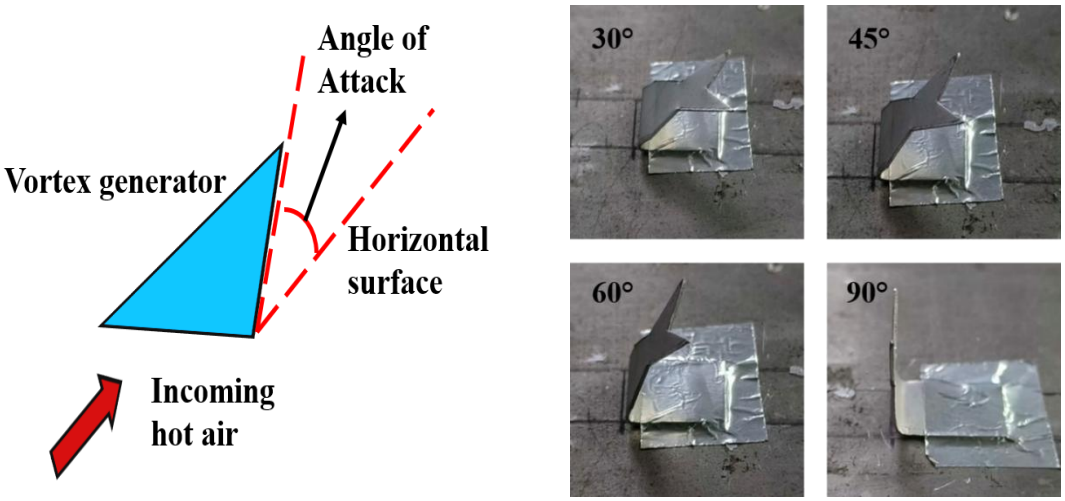

Fig. 3.5 Angle of inclination representation and the angles used in the present study

3.1.2 Mathematical Modeling

The analysis assumes a continuous and incompressible flow with constant thermophysical characteristics of air. The application of Navier-Stokes equations, Fourier's law, and no-slip wall condition are integral to the modeling process. A 1-D thermal resistance model is utilized to evaluate heat transport within the system. The heat exchanger (HX) is divided by flow-direction control units, facilitating the examination of individual interactions that govern bulk phenomena upon the entry of hot gas into the system. Heat transfer through convection occurs as the hot gas releases heat in each control unit, as represented by Eq. (3.1). Thermoelectric generators (TEGs) subsequently conduct and absorb this heat. Upon reaching a stable condition, the energy conservation calculations can be derived for each control system, delineating the heat dissipation within the control unit originating from the hot gas (Q).

$$\dot{Q} = \dot{m}_e * C_{p,e} * (T_{e,1} - T_{e,2}) \tag{3.1}$$

Herein, $C_{p,e,}$ and m_e denote the specific heat capacity and mass flow rate of the hot gas, respectively. The lower surface of the heat exchanger (HX), maintains temperatures within ±0.2°C uniformity. The temperature of the hot gas at a specific site is denoted as $T_{e,i}$. A hole drilled into the plate facilitates the placement of a thermocouple in the trail of the hot gas, allowing for the measurement of the temperature of the i^{th} section. The average control unit temperature can be computed utilizing Eq. (3.2).

$$T_{avg\ 1,2} = \frac{T_{e,1} + T_{e,2}}{2} \tag{3.2}$$

$\dot{Q}$ amount of heat is convected across the heat exchanger. The outside face temperature ($T_{out1,2}$) is measured experimentally, while the inner face temperature ($T_{in1,2}$) remains unknown. At a steady state, convection equals conduction heat transmission (Eq. 3.3). Mathematically,

$$h_{e,1}Ar\left(T_{avg1,2} - T_{in1,2}\right) = \frac{T_{in1,2} - T_{out1,2}}{R_{cond}} \tag{3.3}$$

Where $h_{e,1}$ is the internal convective HTC, and R_{cond} is heat-exchanger wall conduction resistance which is calculated using Eq. 3.4

$$R_{cond} = \frac{t_p}{k_{Al}\, Ar} \tag{3.4}$$

In the context of the Eq. 3.4 provided, Ar, k_{Al}, and t_p denote the cross-sectional area of the unit, the thermal conductivity of aluminum, and plate thickness, respectively. Eqs. (3.1-3.4) collectively determine the convective heat transfer coefficient ($h_{e,i}$) for each control volume. Consequently, the approximation of the typical internal HTC ($h_{avg,e}$) for the heat exchanger is derived as depicted in Eq. (3.5).

$$h_{avg,e} = \frac{\sum h_{e,i}}{i} \tag{3.5}$$

Here, the variable "i" represents the control unit number. The initial phase of experimentation involves subjecting the heat exchanger's flat internal topology to testing. As delineated in Figs. 4(a) and 4(b), F and D shape VGs are strategically positioned within heat exchangers to conduct a series of iterative trials. Parameters such as distance-to-height ratio and angle of inclination are systematically investigated. The assessment of the heat exchanger's performance is conducted under specific conditions: an airflow rate of 0.0116kg/s, and an ambient temperature of 31°C.

The study employs a 1-D thermal resistance model at steady state to analyze heat transfer on the hot side of the thermoelectric generator (TEG). This model is chosen due to its simplicity, computational efficiency, and effectiveness in capturing the key heat transfer mechanisms involved. The thermal resistance approach allows for a clear representation of heat flow through different layers, including convective heat transfer from hot air to the heat exchanger’s inner walls, conductive heat transfer through the

exchanger material, and further convection to the TEG surface. By using a steady-state assumption, the model simplifies complex transient effects, making it suitable for evaluating the overall thermal performance under stable operating conditions. This method provides an efficient way to quantify heat transfer rates and temperature gradients, which are critical for optimizing the heat exchanger design and improving TEG efficiency. The key assumptions in this work—like steady-state operation and constant material properties—were chosen for this reason. For instance, assuming a steady state means we analyzed the system when it was running steadily, not while it was starting up or changing speed. The experimental setup was run long enough so that the changes in the parameters being measured were negligible with time. This is a common approach that lets us clearly compare the performance of different designs. Similarly, assuming that properties like conductivity don't change with temperature greatly reduces calculation time while still providing accurate comparative results. This assumption is also considered as the properties do not vary drastically within the working range of the studies.

The power output of TEG can be determined using the correlation expressed as Eq. (3.6):

$$Power = K(\Delta T)^2 \tag{3.6}$$

Here, K = 0.002W/K^2 is a constant specified by the manufacturer, with the atmospheric temperature prevailing on the cold side. In heat transfer applications, friction factor holds significance, unswervingly influencing pressure drop. Eq. 3.7 determines the friction factor for a channel with an even cross-section:

$$f = \frac{(\Delta P/L)D_h}{(\rho V^2/2)} \tag{3.7}$$

Where ΔP, L, and D_h denote the pressure drop, channel length, and hydraulic diameter respectively. The thermal-hydraulic performance is expressed by TEF, as calculated by the relation in Eq. (3.8) (Karana and Sahoo, 2020):

$$TEF = \frac{\frac{Nu}{Nu_o}}{\left(\frac{f}{f_o}\right)^{1/3}} \tag{3.8}$$

The uncertainty (Kline and Mcclintock, 1953) in the determined constraints is computed utilizing the relation specified by the source referenced as:

$$U_F = \sqrt{\left(\frac{\partial F}{\partial x_i}U_1\right)^2 + \left(\frac{\partial F}{\partial x_i}U_2\right)^2 + \left(\frac{\partial F}{\partial x_i}U_3\right)^2 + \left(\frac{\partial F}{\partial x_i}U_4\right)^2 + \cdots} \tag{3.10}$$

Table 3.1 presents the maximum indecision associated with the measured parameters.

Table 3.1: Uncertainty of parameters used in the study

Parameter	Maximum Uncertainty
Dimension measurement	±1mm
Temperature	$\pm 0.1^0$C
Velocity	±0.1m/s
Heat transfer coefficient	2.96%
Heat transfer rate	2.19%
Pressure drop	±1mm

The relative errors in different parameter utilized in the study are as follows:

$$\frac{\partial Ar}{\Delta Ar} = \pm 0.01$$

$$\frac{\partial T}{T} = \pm 0.01$$

$$\frac{\partial v}{v} = \pm 0.01$$

$$\frac{\partial \dot{m}}{\dot{m}} = \pm 0.05$$

$$\frac{\partial \Delta P}{\Delta P} = \pm 0.01$$

$$\frac{\partial TEF}{TEF} = \pm 0.1$$

$$\frac{\partial Power}{Power} = \pm 0.01$$

3.2 Results and Discussion

3.2.1 Effect of vortex generators on the heat transfer coefficients

Figs. 3.6 (a-d) show heat transfer coefficient variation for different configurations along the length of the HX. The enhancement in the heat transfer coefficient with the incorporation of vortex generators in the heat exchanger is primarily attributed to the induced secondary flow structures that promote fluid mixing. Vortex generators disrupt the boundary layer, generating longitudinal vortices that increase turbulence intensity and enhance convective heat transfer. These vortices transport higher-momentum fluid from the core region toward the heat exchanger walls, thereby increasing the local heat transfer coefficient. Additionally, the breakdown of the thermal boundary layer due to vortex shedding facilitates better energy exchange between the hot air stream and the heat exchanger surface. Furthermore, it has been reported previously that vortex generator inserts are capable of production of local heat transfer enhancement (Deshmukh et al., 2016). Previous study (Pal et al., 2012) have also reported a significant enhancement in heat transfer because of the strong swirling motion originating from the streamwise longitudinal vortices behind the pair of delta winglets.

The observation that a distance-to-height (D/H) ratio of 2 results in the highest heat transfer coefficient across all vortex generator configurations is linked to the optimal interaction of vortices along the channel. At this spacing, the vortices retain their strength and effectively merge, sustaining a high level of turbulence and enhancing thermal mixing. When the D/H ratio increases beyond this value, the vortices tend to dissipate before interacting effectively with the subsequent vortex structures, leading to reduced enhancement. Conversely, at lower D/H ratios, excessive vortex interactions may induce flow recirculation and pressure losses, diminishing the convective heat transfer efficiency.

The superior performance of the fishtail vortex generator (FVG) compared to the M-envelope and delta vortex generators can be attributed to its distinctive aerodynamic shape, which generates stronger and more stable vortex structures. The fishtail configuration likely promotes the formation of larger coherent vortices that persist over a longer streamwise distance, thereby ensuring sustained enhancement in convective heat transfer. Moreover, the shape may also contribute to a more uniform velocity profile, reducing flow separation and minimizing pressure losses while maximizing heat transfer augmentation.

The inclination angle of 60° yielding the highest heat transfer coefficient can be explained through the balance between vortex strength and aerodynamic resistance. At lower inclination angles (e.g., 30 and 45°), the vortex generators induce weaker vortices due to a reduced flow disturbance, limiting their effectiveness in enhancing thermal transport. Conversely, at a high inclination of 90°, the vortex generators create significant flow resistance and excessive separation, leading to high-pressure drop penalties and flow stagnation, which counteract the heat transfer benefits. The 60° inclination provides an optimal orientation where the induced vortices are both strong and stable, maximizing turbulent energy transport while maintaining a favorable pressure drop-to-heat transfer

trade-off. This inclination ensures effective boundary layer disruption without introducing excessive drag, leading to the highest observed heat transfer coefficient.

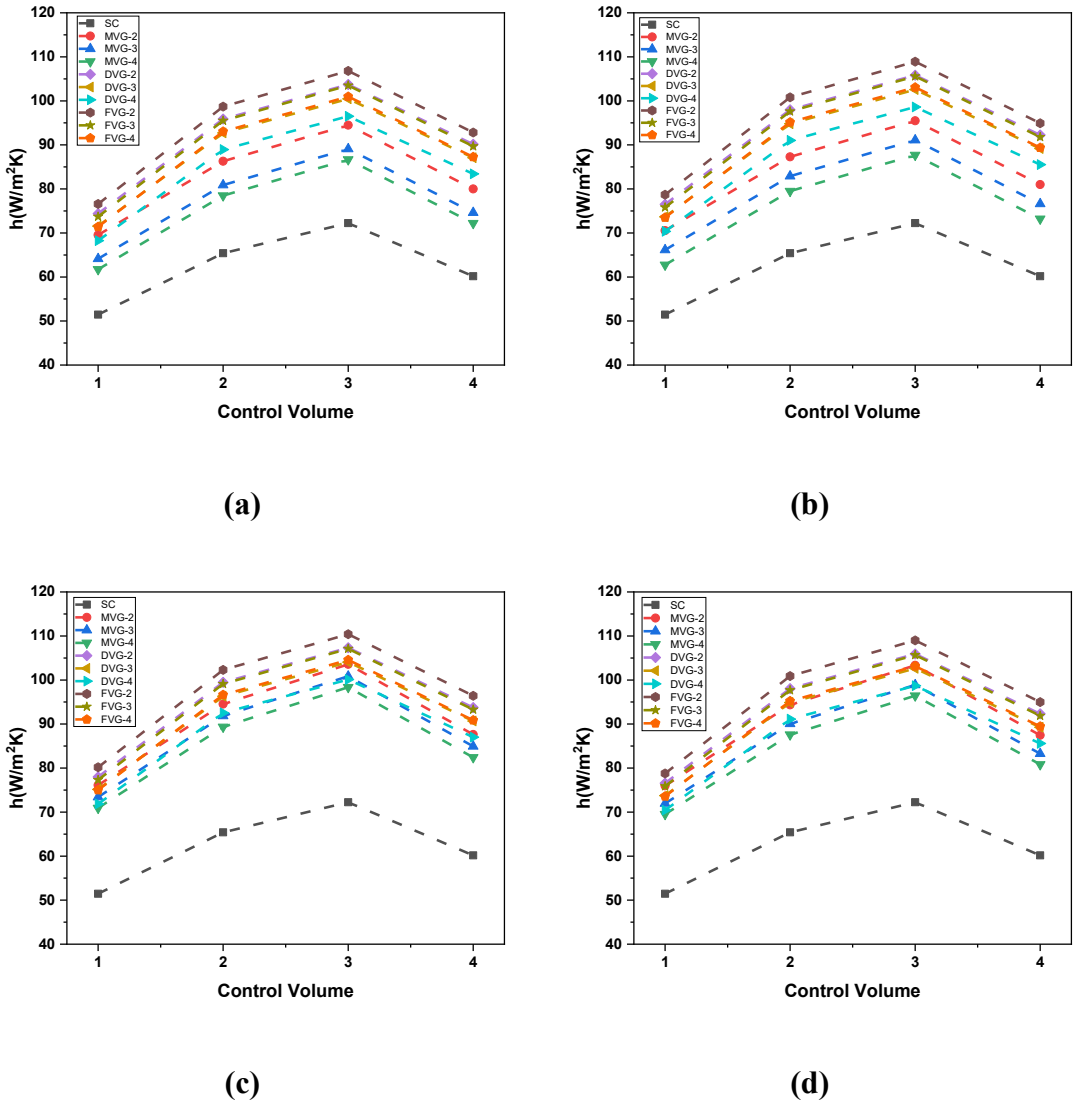

Fig. 3.6 Heat transfer coefficient with control volume for different VG shapes and D/H ratios at angles of inclination of (a) 30°, (b) 45°, (c) 60°, and (d) 90°

Further analysis depicts that the initial increase in the heat transfer coefficient with control volume number is attributed to the progressive development and intensification of secondary flow structures induced by the vortex generators. As the hot air flows downstream, these vortices fully form, efficiently disrupting the thermal boundary layer and generating significant turbulence. This enhances fluid mixing, transporting high-

momentum fluid from the core toward the walls and substantially boosting convective heat transfer. The subsequent decrease beyond the third control volume occurs due to vortex decay and dissipation downstream. Consequently, this leads to increased thermal resistance and a decline in the local heat transfer coefficient along the remaining length of the heat exchanger.

3.2.2 Effect of vortex generators on the pressure drops

Figs. 3.7 (a-d) show the pressure drops for different configurations along the length of the HX. The pressure drop in the heat exchanger is observed to be higher at lower D/H ratios due to the increased number of vortex generators within the flow domain. A lower D/H ratio implies that the spacing between consecutive vortex generators is reduced, leading to a greater number of flow obstructions along the channel. This intensified obstruction enhances flow resistance, causing a higher pressure loss. Additionally, the increased frequency of vortex shedding and secondary flow interactions leads to elevated turbulence levels and greater energy dissipation, further contributing to the rise in pressure drop. Moreover, excessive vortex interactions in tightly spaced configurations can induce flow recirculation zones, increasing overall flow resistance and pressure losses. The fishtail vortex generator exhibits the lowest pressure drop among the tested configurations due to its aerodynamic shape, which facilitates smoother airflow deflection with minimal abrupt separations. Unlike M-envelope and delta vortex generators, the fishtail design likely generates weaker trailing vortices, leading to a more streamlined flow pattern. This reduces flow separation and pressure drag, resulting in lower energy dissipation. Furthermore, the fishtail configuration may encourage a more gradual redistribution of flow momentum, preventing excessive turbulence generation while still promoting effective heat transfer enhancement.

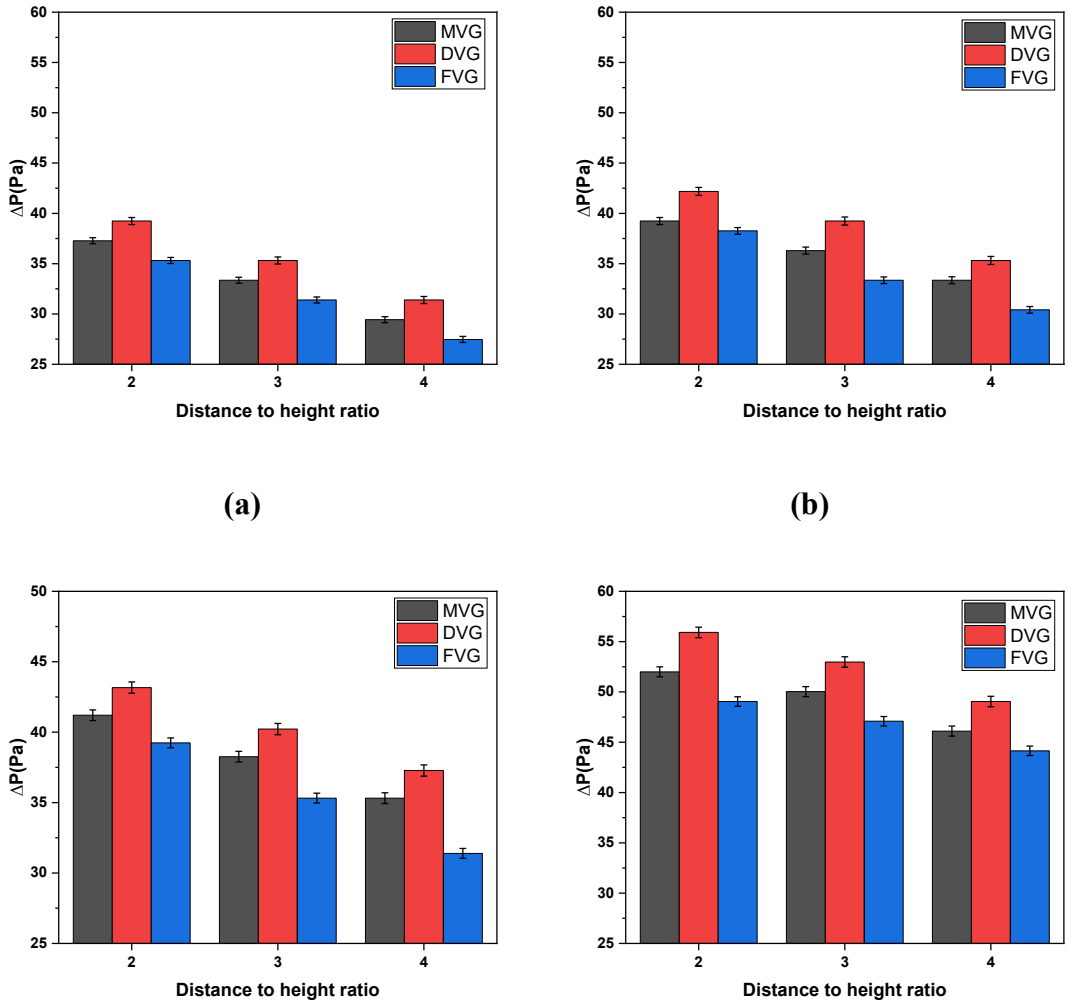

Fig. 3.7 Pressure drops for different VG shapes and D/H ratios at angle of inclination of (a) 30°, (b) 45°, (c) 60°, and (d) 90°

The highest pressure drop is observed when the vortex generators are inclined at 90°, which is attributed to the substantial obstruction posed by the incoming hot air stream. At this inclination, the vortex generators act as perpendicular barriers to the flow, causing significant flow separation and wake formation. This increased blockage effect leads to stronger vortex shedding, high turbulence intensity, and pronounced flow stagnation, all of which contribute to a considerable rise in pressure drop. Additionally, the abrupt deflection of the airflow at a steep inclination results in greater momentum losses and increased form drag, further elevating the pressure loss in the system.

3.2.3 Effect of vortex generators on thermal enhancement factors

Figs. 3.8 (a-d) show TEF for different configurations along the length of the HX. The increase in the thermal enhancement factor (TEF) with the D/H ratio can be attributed to the more favorable balance between heat transfer enhancement and pressure drop penalty at the larger spacing between vortex generators. As the D/H ratio increases, the interaction between consecutive vortices is optimized, reducing excessive flow disturbances and minimizing unnecessary energy dissipation. While the heat transfer coefficient may exhibit a gradual decline at higher D/H values due to weaker vortex interactions, the corresponding reduction in pressure drop leads to a lower friction factor. Since TEF is defined as a ratio that penalizes excessive pressure drop, the reduction in flow resistance at larger D/H ratios results in a net increase in TEF, making the enhancement technique more efficient.

The fishtail vortex generator (FVG) exhibiting the highest TEF value is primarily due to its superior aerodynamic design, which achieves a higher heat transfer enhancement with minimal flow resistance. The fishtail shape likely promotes the generation of stable, coherent vortices that persist over a longer streamwise distance, ensuring sustained convective heat transfer augmentation. Simultaneously, its streamlined configuration minimizes abrupt flow separations and recirculation zones, leading to a lower friction factor compared to M-envelope and delta-shaped vortex generators. This optimal balance between thermal augmentation and pressure drop reduction makes the FVG the most efficient configuration, as reflected in its highest TEF value.

The lowest TEF value at an inclination angle of 90° can be attributed to the excessive obstruction caused by the vortex generators, leading to a disproportionately high-pressure drop relative to the achieved heat transfer enhancement. At this inclination,

the vortex generators act as nearly perpendicular barriers to the incoming hot air stream, significantly disrupting the flow dynamics. While the presence of strong vortices at this angle enhances localized convective heat transfer, the induced pressure drop becomes excessively high due to increased frictional and form drag. The large-scale recirculation zones and intensified turbulence further contribute to energy dissipation, which negatively impacts the overall thermohydraulic performance.

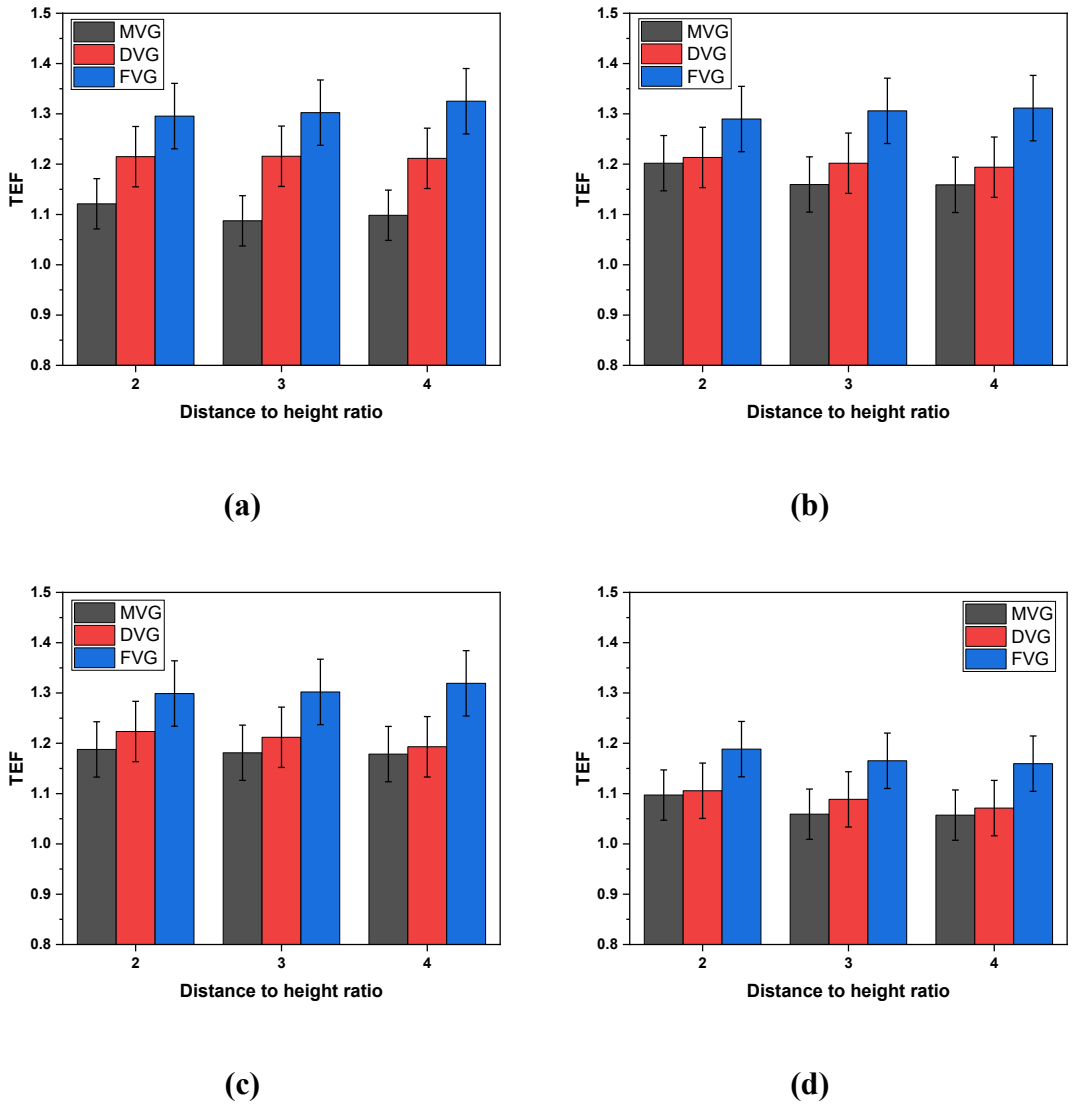

Fig. 3.8 Thermal enhancement factors for different VG shapes and D/H ratios at angle of inclination of (a) 30°, (b) 45°, (c) 60°, and (d) 90°

Consequently, despite a possible improvement in the heat transfer coefficient, the substantial increase in flow resistance leads to a sharp decline in the thermoelectric performance factor (TEF). Since TEF is a measure that integrates both heat transfer augmentation and pressure drop penalties, the severe aerodynamic resistance at 90° results in an unfavorable trade-off. The excessive pressure drop diminishes the net energy gain, making this configuration the least efficient in terms of overall performance. The quantitative evaluation of these effects, including variations in TEF, friction factor, and heat transfer coefficient, is systematically presented in Table 3.2 for comprehensive analysis.

Table 3.2: Percentage variation of different thermohydraulic parameters for different Vortex generator configurations with smooth channel as the reference

θ	D/H ratio	Average HTC			ΔP			TEF		
		MVG	DVG	FVG	MVG	DVG	FVG	MVG	DVG	FVG
30°	2	32.5	46.0	50.4	65.2	73.9	56.5	12.1	21.4	29.5
	3	23.8	41.1	45.3	47.8	56.5	39.1	8.7	21.5	30.2
	4	20	35.2	41.4	30.4	39.1	21.7	9.8	21.1	32.5
45°	2	44.5	49.4	53.7	73.9	86.9	69.5	20.1	21.3	28.9
	3	35.8	44.5	48.7	60.8	73.9	47.8	15.9	20.1	30.5
	4	32	38.6	44.8	47.8	56.5	34.7	15.8	19.4	31.1
60°	2	45.1	51.8	56.1	82.6	91.3	73.9	18.7	22.3	29.8
	3	40.8	46.9	51.1	69.5	78.2	56.5	18.1	21.1	30.2
	4	36.8	41.0	47.2	56.6	65.2	39.1	17.8	19.3	31.9
90°	2	44.8	49.5	53.9	130.4	147.8	117.3	9.7	10.5	18.8
	3	38.0	44.6	48.8	121.7	134.7	108.6	5.9	8.8	16.5
	4	34.1	38.7	44.9	104.3	117.3	95.6	5.7	7.1	15.9

3.2.4 Effect of vortex generators on TEG power output

Figs. 3.9 (a-d) show the average TEG power output for different configurations along the length of the HX. The observed decrease in TEG power output with increasing D/H ratio can be attributed to the corresponding reduction in the heat transfer coefficient. At lower D/H ratios, the closely spaced vortex generators induce stronger vortical structures, enhancing fluid mixing and increasing convective heat transfer rates at the hot-side surface of the heat exchanger. This leads to a higher outer surface temperature, thereby maximizing the temperature gradient across the thermoelectric generator. However, as the D/H ratio increases, the spacing between vortex generators grows larger, weakening vortex interactions and reducing convective augmentation. Consequently, the heat exchanger surface temperature declines, thereby diminishing the temperature difference available for thermoelectric power generation, leading to a drop in TEG power output.

The highest TEG power output observed for the heat exchanger equipped with fishtail vortex generators (FVG) can be explained by the superior thermal performance of this configuration. The fishtail shape promotes strong and persistent vortices, ensuring an effective enhancement of heat transfer while simultaneously maintaining a relatively lower pressure drop. This results in a higher surface temperature of the heat exchanger, leading to an increased temperature differential across the thermoelectric generator. Since TEG output is directly proportional to the temperature difference between its hot and cold sides, the improved convective heat transfer efficiency of FVG-equipped heat exchangers translates into superior TEG power generation compared to M-envelope and delta-shaped vortex generators.

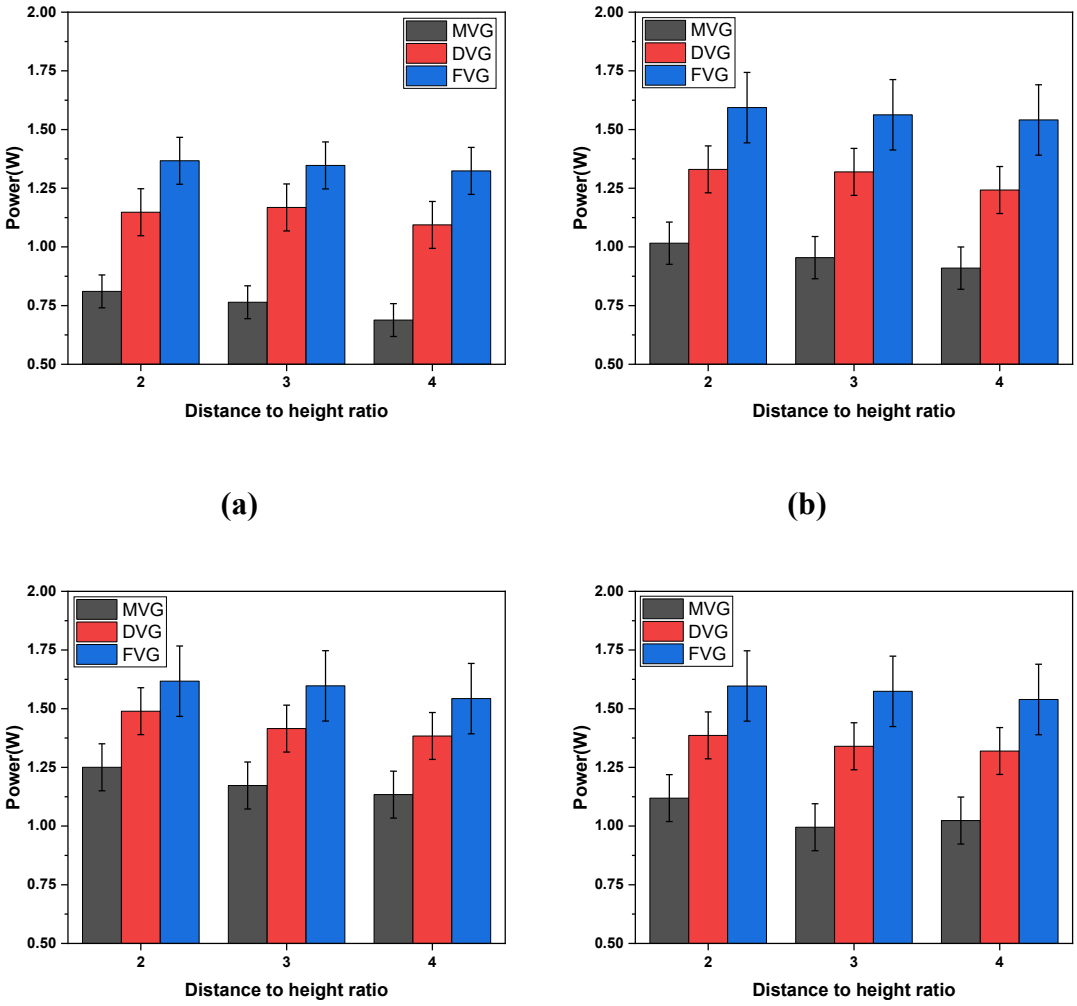

Fig. 3.9 TEG power output for VG shapes and D/H ratios at angle of inclination of (a) 30°, (b) 45°, (c) 60°, and (d) 90°

The trend of increasing TEG power output with an inclination angle up to 60°, followed by a decline at 90°, is governed by the interplay between heat transfer enhancement and flow resistance. At lower inclination angles, the vortex generators generate moderate yet effective vortices, improving convective heat transfer and raising the heat exchanger surface temperature, which in turn boosts TEG power. As the inclination reaches 60°, vortex strength and interaction reach an optimal state, maximizing heat transfer augmentation and, consequently, TEG power output. However, at 90°, the vortex generators act as significant obstructions to the airflow, causing

excessive pressure losses and flow stagnation, which disrupts efficient convective heat transfer. This leads to a reduction in the heat exchanger surface temperature, thereby diminishing the temperature gradient available for TEG power generation. Thus, the decrease in TEG power at 90° is primarily due to the adverse effects of increased flow resistance and disrupted thermal transport mechanisms.

3.3 Highlights

- Vortex generators create longitudinal vortices that enhance fluid mixing. This improves heat transfer by disrupting the boundary layer and bringing hotter fluid closer to the cooler surface. By improving mixing, VGs help achieve a more uniform temperature profile across surfaces, which is beneficial in heat exchangers.
- The maximum increment in heat transfer coefficients are 45.16%, 51.85%, and 56.18% for MVG, DVG, and FVG respectively at D/H=2 and θ=60°.
- The vortex generators come with a penalty in the form of increased pressure drop which is high at a lower D/H ratio and high inclination angle because of the increase in obstruction to hot air flow. The highest pressure drops obtained are 3.46Pa, 3.72Pa, and 3.27Pa for MVG, DVG, and FVG respectively at D/H=2 and θ=90°.
- The heat exchanger equipped with vortex generators gives a thermal enhancement factor greater than 1 which depicts that placement of VGs for waster heat recovery through TEG is successful.
- The TEG output improved due to higher surface temperature in channels equipped with VGs than the smooth channel, owing to better heat transfer. The highest average TEG power obtained is 1.62W.

- Vortex generators have the capacity to improve TEG performance as well as support in reducing the size of the waste heat recovery systems.